Innovative Computing Review (ICR)
Volume 4 Issue 1, Spring 2024
$ISSN_{(P)}$: 2791-0024, $ISSN_{(E)}$: 2791-0032
Homepage: https://journals.umt.edu.pk/index.php/ICR

Article QR

Title: **Fractal View and Thermal Behavior of Fractional Metallic Porous Fins in Response to Changing Convective Conditions**

Author (s): H. M. Younas, M. Mohy-U-Din Liaqat, Shahzad Anjum, Emaan Afzal, Sumbal Shahzadi, and Reha Salman

Affiliation (s): Riphah International University, Faisalabad, Pakistan

DOI: https://doi.org/10.32350/icr.41.05

History: Received: March 22, 2024, Revised: April 09, 2024, Accepted: May 25, 2024, Published: June 10, 2024

Citation: H. M. Younas, M. M.-U-D. Liaqat, S. Anjum, E. Afzal, S. Shahzadi, and R. Salman, "Fractal view and thermal behavior of fractional metallic porous fins in response to changing convective conditions," *Innov. Comput. Rev.*, vol. 4, no. 1, pp. 70–83, June 2024, doi: https://doi.org/10.32350/icr.41.05

Conflict of Interest: Author(s) declared no conflict of interest

A publication of
School of Systems and Technology
University of Management and Technology, Lahore, Pakistan

Fractal View and Thermal Behavior of Fractional Metallic Porous Fins in Response to Changing Convective Conditions

Hafiz Muhammad Younas*, Muhammad Mohy-U-Din Liaqat, Shahzad Anjum, Emaan Afzal, Sumbal Shahzadi, and Reha Salman

RIPHAH International University, Faisalabad, Pakistan

ABSTRACT Porous, permeable, and structured fins enhance heat transfer due to their thermophysical properties. Understanding the thermal gradients in these fins is critical for a variety of engineering applications. This study applies the Homotopy Perturbation Method (HPM) to nonlinear fractional differential equations describing porous fins, focusing on factors such as porosity, permeability, and convection. Thermal analysis with an insulated tip of a copper alloy reveals that porosity has the greatest impact on heat transfer. The study highlights the effectiveness of HPM in analyzing these thermal systems. The system's porosity is found to be more influential than any other factor.

INDEX TERMSconvection, heat transfer, fins, fractional analysis, Homotopy Perturbation Method (HPM), permeability, porous, thermal.

I. INTRODUCTION

The investigation of thermophysical properties in convective flow through a porous permeable medium is crucial for various engineering challenges. Porous permeable metallic and ceramic materials find extensive industrial and biomedical applications. Their potential as advanced materials is evident due to their wide range of uses. Numerous mathematical and experimental studies have been conducted to provide a deeper understanding of the mechanisms of heat transfer within porous permeable media. Such media have numerous applications including catalytic bed reactors, enhancing drying efficiency, filtration, separation, and petroleum recovery processes. Thermionic conductive porous permeable materials are utilized to improve forced convective heat transfer in various technological applications, such as reactor design, thermal components including heat exchangers, and parabolic solar plate heaters [1]–[5].

Swift advancement of electronic equipment has led to significant developments in these areas. In various manufacturing, business, and ecological enterprises, advancements have been paralleled by improvements in heat dissipation (cooling) methods. Enhancing natural convection has been, and will remain, essential to optimize the performance of heat dissipation systems in integrated circuit technology. A wonderful functional element to improve heat transmission from the heated areas and surfaces is a fin or stretched surface. It has been widely used in automobiles, heat transfer equipment, and atmospheric heat conditioning, among other applications. Several studies have aimed to eliminate the fin-based system's material cost and dimensional/geometrical viewpoints [3]–[8]. The improvement of heat dissipation in extended surfaces or fins has been focused in research and development, leading to the exploration of porous fins. This area of study has seen extensive investigation into the use of porous finned structures (PFS).

*Corresponding Author: hmy.maths@gmail.com

Two key factors in these systems are permeability (which refers to the interconnectivity and scale of the pores in PFS) and the convective load. [7], [8] conducted a preliminary investigation on heat transfer in fins. They studied the heat transfer characteristics of fins and found that using porous fins enhances heat transfer due to their geometrical advantages. Such fins can improve heat dissipation for a given area while reducing material mass by incorporating holes and cavities. It is important to note that Kiwan and Al-Nimr [9] were the first to propose the concept of using porous fins to enhance heat dissipation. Additionally, Kiwan [10] introduced the Darcy approach to model the solid-gas/air interfaces in porous fin structures. Khaled [11] investigated heat dissipation in quadrangular porous fins and found that these fins improved the heat dissipation rate. Kiwan and Zeitoun [12] demonstrated that cylindrical porous fins enhance thermionic transitions. Ghasemi et al. [13] also contributed to this field. Kiwan [14] examined the impact of thermionic radiation on heat dissipation in PFS. E. Cuce and P. M. Cuce [15] effectively utilized HPM to evaluate the efficiency and performance of quadrangular permeable fins. Ma et al. [16] employed a numerical approach to study the thermal capacity of convective-radiative permeable fins. Moradi et al. [17] used an HPM model to analyze convective capacity and thermal dissipation in movable porous permeable fins. Bhanja et al. [18] developed an analytical model to determine fin performance and optimize geometric design constraints for a movable porous-structured fin in a convective-radiative environment. Additionally, Das [19] validated the inverse results of the convection-radiation approach for cylindrical porous permeable fins. Numerous applications are related to the parameters of permeability, porosity, and internal heat evolved/generated in the system.

The properties of the linked solid components and the fluids contained in porous membranes and structures have been used to examine the various physiothermal characteristics of such structures in metals and ceramics [20]–[29]. A comprehensive overview of convective heat transfer of nanofluids in porous media is given by Mohammad Hemmat Esfe et al. [30]. Liaqat Ali et al. [31] investigated the thin-film flow of a magnetohydrodynamic (MHD) fluid over a porous, constantly stretching surface with a magnetic field and radioactive heat fluctuation in the presence of thermal conductivity and variable viscosity. L. Ndlovu [32] examined the temperature distribution and fluctuation and fin efficiency in a porous moving fin of a rectangular partner. Fractional calculus, encompassing the concepts of nonintegral order differentiation and integration, extends the principles of classical calculus. Over recent years, numerous mathematicians, researchers, and scientists have recognized the significant role of non-integer operators in describing the characteristics of various physical phenomena [33]–[37]. Fractional differentiation and integration have been effectively employed to elucidate many procedures and apparatus. Comparative studies between classical models and fractional models have been conducted extensively [20]–[25]. HPM has emerged as a rapidly convergent technique, compared to others. Its reliability and effectiveness have been well documented in literature across diverse applications in science and engineering. This paper is divided into four sections. Section 2 formulates the governing equation based on the heat transfer equation. Section 3 provides computational remarks for the solution using HPM.

II. GOVERNING EQUATION

In this study, a quadrangular fin contour, as illustrated in Figure 1, has been chosen to analyze the behavior of convective effects. The system's convection is described using a differential equation. The geometric dimensions of the fin are specified as follows: length is represented by "L," width by "w," and thickness by "t." The fin's cross-sectional area remains constant and is not subject to variation. Due to its distinctive porosity, the heat stream can flow through this fin. The system is analyzed using Darcy's porous-medium approach and the total energy balance of the system is represented as follows:

$$q(x) - q(x + \Delta x) + q * A\Delta(x) = m * C(p)[\tau - \tau\infty] + h(p)\,\Delta x\,[\tau - \tau\infty]. \quad (1)$$

In contrast, the mass flow rate of the convective fluid streaming PFS is given as follows:

$$m * = \rho.v.w(x) \triangle (x). \quad (2)$$

Velocity as flow-steam is given as follows:

$$\mathrm{Uw} = \frac{gk\beta(\tau-\tau\infty)}{U}. \quad (3)$$

It is assumed in this system that the fin's heat energy changes with temperature. Here, the steady state condition is determined using the idea of energy balance

$$\frac{d^{\alpha}U}{d\,x_{\alpha}} - ShU^2(x) - m^2U(x) + m^2G(1 + \varepsilon U) = 0, \quad (4)$$

where

$$U = \frac{(\tau - \tau\infty)}{(\tau b - t\infty)}\ And\ X = \frac{x}{L}. \quad (5)$$

Porous value $S_k = \frac{D_a R_a}{k}\left(\frac{L}{t}\right)$, while the convection parameter $m = \left(\frac{h_P}{k_A}\right)^{\frac{1}{2}}$. In this case, S is a porosity-related metric that describes the buoyancy effect and the porous structure's permeability. The larger interconnected porousness of PSF or larger buoyantic forces are indicated by a higher value of Sh. The result of convection from the fin's surface is indicated by the convective parameter m. The requirements for the task are for a fin of finite length with an insulated tip $U(0) = 1,\ \frac{dU}{dx}|_{X=1} = 0$.

The perturbation approach has been used with the concept of homotopy to tackle non-linear issues. Kiwan and Al-Nim [9] carried out an investigation by applying HPM. Marinca et al. developed a unique method that they call HPM [29]. HPM has the advantage of establishing its convergence criteria more pliably than HAM. The three-dimensional (3D) analysis for Casson-nanofluid and Carreau-nanofluid flows caused by a flat body in MHD flow is provided by R. Kumar [38]. HPM is used by Nawaz *et al.* [39] to solve a linked system of nonlinear partial differential equations (PDEs). [40]–[44] demonstrate the value, generalizability, and reliability of this approach in a number of publications. They also produce solutions that can be relied upon and provide significant applications in science and engineering. This study presents an articulated concept of HPM. It offers rational and reliable solutions to PDEs and differential equations that are time-dependent, linear, non-linear, and fractional in space and time.

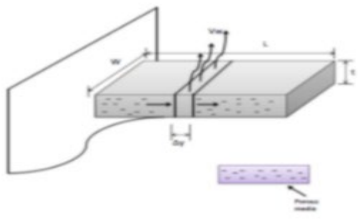

Fig 1. Sketch of porous fin structure

III. BASIC DEFINITIONS OF FRACTIONAL CALCULUS

We provide some elementary definitions of real valued functions in this section. A real-valued function $f(t)$, where $t > 0$, is defined as follows: c_{μ}, $\mu \in R$. Precisely defined as [44], [45],

$$f(t) = t^{p} f_1(t),$$

where $f1(t) \in c(0,\infty)$ is presumed to be in space c_{μ}^{m} if and only if

$$f^{m} \in c_{\mu}, m \in N.$$

The fractional order $\alpha > 0, \mu \geq -1$ Riemann-Liouville sense integral operator of a function $f \in c_{\mu}$ is defined as

$$RL_{D}{}^{-\alpha}_{a,t} f(t) = \frac{1}{\Gamma(\alpha)} \int_a^t (t - \mu)^{\alpha-1} f(\mu)\, d\mu, t > 0, a \quad 0, k-1 < \alpha < k, k \in Z^{+}. \quad (6)$$

For a function f(t) of fractional order α > 0, the Riemann-Liouville sense derivative operator is defined as

$$RL_{D}{}^{\alpha}_{a,t} f(t) = \frac{1}{\Gamma(n-\alpha)} \frac{d^k}{dt^k} \int_a^t (t - \mu)^{k-\alpha-1} f(\mu)\, d\mu, a > 0, t > 0, k-1 < \alpha < k, k \in Z^{+}. \quad (7)$$

Caputo sense derivative operator of a function f(y) of fractional order α > 0 is defined as

$$C_{D}{}^{\alpha}_{a,t} f(t) = \frac{1}{\Gamma(n-\alpha)} \int_a^t (t - \mu)^{k-\alpha-1} f^{k}(\mu)\, d\mu, \alpha > 0, t > 0, k-1 < \alpha < k, k \in Z^{+}. \quad (8)$$

$If\ j-1 < \alpha < j, and\ f \in c_{\mu}^{m}, \mu \geq -1, then$ $RL_{D}{}^{-\alpha}_{a,t}\left(C_{D}{}^{\alpha}_{a,t} f(t)\right) = f(t) - \sum_{i=0}^{j-1} f^{i}(a) \frac{(t-a)^j}{\Gamma(i+1)}, > 0.$ (9)

IV. FRACTIONAL ORDER HEAT TRANSFER MODEL APPLICATIONS

$$\frac{d^{\alpha}U}{dx^{\alpha}} - S_h U^2(x) - m^2 U(x) + m^2 G(1 + \epsilon U) = 0, \quad (10)$$

where $U = \frac{(\tau - \tau\infty)}{(\tau b - t\infty)}$ $and\ X = \frac{x}{L}$,

$$U(0) = 1 \quad , \quad \frac{dU}{dx}|_{x=1} = 0.$$

Using the HPM approach, we can create an ideal homotopy in the given equation as follows:

$$U^{\alpha} + P[-SU^2 - m^2 è + m^2 G(1 + \epsilon U)] = 0. \quad (11)$$

$In\ the\ following, p^0, p^1, p^2, and\ p^3$ are problems of the zeroth, first, second, and third orders.

p^0:

$$\frac{d^{\alpha}U_0}{dx^{\alpha}} = 0 \quad (12)$$

p^1:

$$\frac{d^{\alpha}U_1}{dx^{\alpha}} = S(U_0)(U_0) + m^2 U_0 - m^2 G(1 + \epsilon U_0) \quad (13)$$

p^2:

$$\frac{d^{\alpha}U_2}{dx^{\alpha}} = m^2(U_1) - Gm^2\epsilon(U_1) + 2(U_0)(U_1) \quad (14)$$

p^3:

$$\frac{d^{\alpha}U_3}{dx^{\alpha}} = S(U_1)^2 \quad + \quad +m^2U_2 - Gm^2\epsilon U_2 + 2S(U_0)(U_2) \tag{15}$$

In the following, U_0 , U_1 , U_2, and U_3 are zeroth-order, first-order, and third-order solutions. Using these three solutions in equation 12, we get U solution.

$$U_0 = 1 \tag{16}$$

$$U_1 = \frac{S+m^2(1-G-G\epsilon)}{\Gamma(\alpha+1)}x^{\alpha} \tag{17}$$

$$U_2 = m^2\left[\frac{S+m^2(1-G-G\epsilon)}{\Gamma(2\alpha+1)}x^{2\alpha}\right] -Gm^2\epsilon\left[\frac{S+m^2(1-G-G\epsilon)}{\Gamma(2\alpha+1)}x^{2\alpha}\right] + 2\left[\frac{S+m^2(1-G-G\epsilon)}{\Gamma(2\alpha+1)}x^{2\alpha}\right] \tag{18}$$

$$U_3 = S\left[\frac{S+m^2(1-G-G\epsilon)}{\Gamma(\alpha+1)}\right]^2\frac{\Gamma(2\alpha+1)}{\Gamma(3\alpha+1)}x^{3\alpha} +m^4\left[\frac{S+m^2(1-G-G\epsilon)}{\Gamma(3\alpha+1)}x^{3\alpha}\right] - Gm^2\epsilon\left[\frac{S+m^2(1-G-G\epsilon)}{\Gamma(3\alpha+1)}\right] + 2\left[\frac{S+m^2(1-G-G\epsilon)}{\Gamma(3\alpha+1)}x^{3\acute{a}}\right] \tag{19}$$

$$U = 1 + \frac{2y^{2\alpha}(s+m^2(1-G-G\epsilon))}{\Gamma[1+2\alpha]} + \frac{m^2y^{2\alpha}(s+m^2(1-G-G\epsilon))}{\Gamma[1+2\alpha]} - \frac{Gm^2y^{2\alpha}\epsilon(s+m^2(1-G-G\epsilon))}{\Gamma[1+2\alpha]} + \frac{2y^{3\alpha}(s+m^2(1-G-G\epsilon))}{\Gamma[1+3\alpha]} + \frac{m^4y^{3\alpha}(s+m^2(1-G-G\epsilon))}{\Gamma[1+3\alpha]} - \frac{Gm^2y^{3\alpha}\epsilon(s+m^2(1-G-G\epsilon))}{\Gamma[1+3\alpha]} + \frac{sy^{3\alpha}(s+m^2(1-G-G\epsilon))^2\mathrm{Gamma}[1+2\alpha]}{\Gamma[1+\alpha]^2\Gamma[1+3\alpha]} + \frac{y^{\alpha}(s+m^2[1-G-G\epsilon])}{\Gamma[1+\alpha]} \tag{20}$$

A. RESIDUAL OF FRACTIONAL ORDER METALLIC POROUS FIN ON VARYING CONVECTIVE LOADS

$$R = \frac{d^{\alpha}U}{dx^{\alpha}} - S_hU^2(x) - m^2U(x) + m^2G(1+\epsilon U) \tag{21}$$

B. AVERAGE VELOCITY AND FLOW RATE

$$W = \sum_0^1 u(x)dx$$

$$W = 1 + \frac{s}{\Gamma[2+\alpha]} + \frac{\left(-2+m^2(-1+G\,\epsilon)\right)(-s+m^2(-1+G+G\,\epsilon))}{\Gamma[2+2\,\alpha]} - \frac{(2+m^4-Gm^2\epsilon)\left(-s+m^2(-1+G+G\epsilon)\right)}{\Gamma[2+3\,\alpha]} + \frac{4^{\alpha}\,s\left(s-m^2(-1+G+G\epsilon)\right)^2\Gamma\left[\frac{1}{2}+\alpha\right]}{\sqrt{\pi}\,\Gamma[1+\alpha]\,\Gamma[2+3\,\alpha]} + \frac{m^2(1-G\,(1+\epsilon))}{\Gamma[2+\alpha]} \tag{22}$$

The fractional metallic porous fin on varying convective loads Jeffery-Hamel flow's average velocity $\overline{U}$ Is determined by

$$\bar{u} = \boldsymbol{w}$$

The fractional Jeffery-Hamel flow result, as shown graphically.

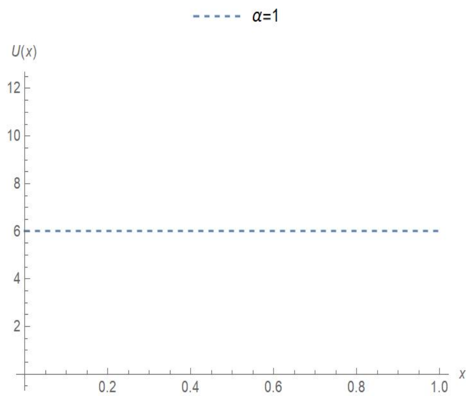

FIGURE 1. The result's behavior observed at $s = 3, G = 0.4, m = 0.1, \in= 0.6, and\ \alpha = 1.$

V. RESULTS AND DISCUSSION

Without using any spatial discretization, the HPM algorithm for the temporal fractional order heat transfer equation described in Sec. 3 and the formulation explanation given in Sec. 4 yield incredibly valid solutions. It is not necessary to compute higher order answers while using HPM. Material property values are derived from [33]. Da = 0.0003; L/t = 10, Ra = 10000, Kr = 954, ε = 0.5, Ks = 411. Tables 2, 4, 6, 8, and 10 represent the approximate results which also represent the validity and accuracy of the method.

A. CASE 1 (DIFFERENT VALUES OF α)

Fractional thermal analysis for α fluctuations is provided in this instance. Regarding 2, $with\, m = 0.1, s = 3, G = 0.4, \in = 0.6$.

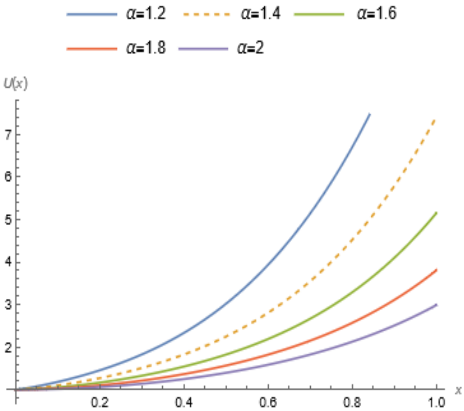

FIGURE 2. 2D Temperature Gradient Analysis for Case 1

TABLE I

RESULTS OF CASE 1 (DIFFERENT VALUES OF α)

X	α = 1.2	α =1.4	α = 1.6	α = 1.8	α = 2
0.1	1.18141663906182	1.0984704278	1.0532846382428	1.0285103606638	1.0150433589880
0.2	1.454156682204560	1.2713641407	1.1650490167101	1.1003435974915	1.0604889697639
0.3	1.826278280854757	1.5095481482	1.3264887670270	1.2118930395974	1.1373676284255
0.4	2.332170890627507	1.8269586813	1.5420107346364	1.3649270693253	1.247677977344
0.5	3.016423605847851	2.2482467334	1.8232366180731	1.5649264368583	1.3948074784765
0.6	3.931330828423049	2.8073040662	2.1887805960676	1.8214901935378	1.584121776004
0.7	5.135830421546348	3.5469882460	2.6648158229219	2.1491817538552	1.8237224482930
0.8	6.694882891059962	4.5191565779	3.2858657279452	2.5685834056658	2.1253731491840
0.9	8.679044449553565	5.7847993381	4.0956729919871	3.1074860593097	2.5055941386030
1	11.164144846878668	7.4142059099	5.1480952315169	3.8021821809219	2.9869252025

TABLE II

RESULTS OF CASE 2 (DIFFERENT VALUES OF ∈)

X	ϵ = 0.2	ϵ = 0.4	ϵ = 0.6	ϵ = 0.8	ϵ = 1
0.1	1.246171036091	1.1326976308343	1.0715759160454	1.0382137470857	1.0201249365328
0.2	1.630274209212	1.3687350143266	1.2223267972172	1.1346168755348	1.0809453437043
0.3	2.188825094631	1.7044746144583	1.4429212958127	1.2850210971390	1.1839957080697
0.4	3.003056035754	2.1741481263384	1.7449888973438	1.4936456415518	1.3324924866776
0.5	4.175719791817	2.8338715761896	2.1543086887152	1.7717558733778	1.5323225762543
0.6	5.826865697324	3.7601244220463	2.7116666124526	2.1392060551031	1.7934271700622
0.7	8.091812826761	5.0497513307491	3.4747142455356	2.6266805857285	2.1315810024318
0.8	11.11986699685	6.8203218331082	4.5200857922846	3.2783087802730	2.5705669809675
0.9	15.07339357763	9.2105830090151	5.9455845125925	4.1545449301636	3.1447462064277
1	20.12709603131	12.380926140017	7.8723761260065	5.3352630527308	3.9020233802777

B. CASE 2 (DIFFERENT VALUES OF ∈)

In this case, fractional thermal analysis for variations in ∈ is given. $For\ \in=1\ with\ m=0.3, s=4, G=0.4, \alpha=1.4.$

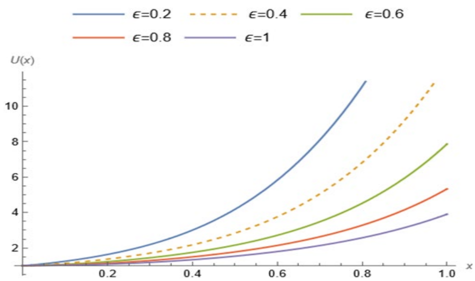

FIGURE 3. 2D Temperature Gradient Analysis for Case 2

C. CASE 3 (DIFFERENT VALUES OF G)

In this case, fractional thermal analysis for variations in G is given. For G=1 with m=0.3, s=5, ∈=0.6, $\alpha=1.4$

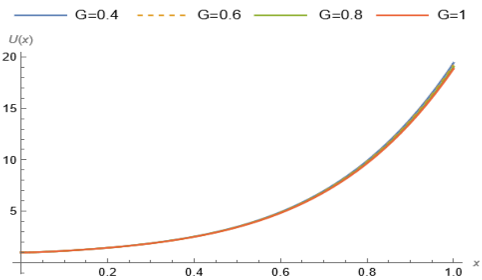

FIGURE 4. 2D Temperature Gradient Results for Case 3

TABLE III
RESULTS OF CASE 3 (DIFFERENT VALUES OF G)

X	= 0.4	= 0.6	= 0.8	= 1
0.1	1.16653535378245	1.1645948744811394	1.1636250249942968	1.1626554356166625
0.2	1.467043938730760	1.4613146182142676	1.4584535326313142	1.4555948301652226
0.3	1.910296468580126	1.8982678908884087	1.8922680098111981	1.8862777339130858
0.4	2.563543874724515	2.5410409277095947	2.529830108296882	2.518646391614001
0.5	3.533476230842525	3.4938352155470347	3.4741080242660383	3.4544430438962057
0.6	4.965047416136141	4.8982796898985335	4.865082685257754	4.832010252935658
0.7	7.042067895942152	6.933996549445583	6.880300256272839	6.826830216483786
0.8	9.988155594407614	9.819524485829396	9.735781693331614	9.652420742028042
0.9	14.06773941802519	13.813296279039129	13.686987500041873	13.561287248041793
1	19.58703234799686	19.214588000396848	19.02975509653562	18.845848372633565

D. CASE 4 (DIFFERENT VALUES OF m)

In this case, fractional thermal analysis for m fluctuations is provided. Regarding $m=0.4\ with\ G=0.4, s=3, \in=0.6, \alpha=1.6.$

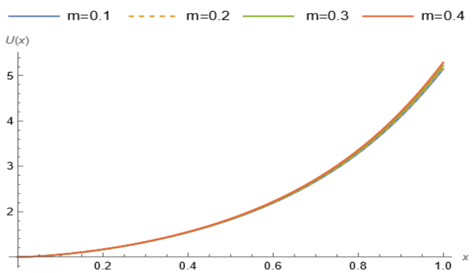

FIGURE 5. 2D Temperature Gradient Results for Case 4

E. CASE 5 (DIFFERENT VALUES OF S_h)

In this case, fractional thermal analysis for fluctuations in S is provided.

For S of 5 with $G=0.4, m=0.3, \in=0.6, \alpha=1.4.$

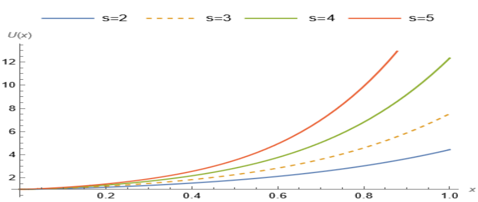

FIGURE 6. 2D Solutions of Case 4 Showing Temperature Variations with Different S_h Values

TABLE IV

RESULTS OF CASE 4 (DIFFERENT VALUES OF m)

X	m = 0.1	m = 0.2	m = 0.3	m = 0.4
0.1	1.0532846382428058	1.0534818890689195	1.0538107327553794	1.0542713078505557
0.2	1.1650490167101466	1.1656956791645614	1.1667743595732327	1.168286424752145
0.3	1.3264887670270018	1.327863519888187	1.330158410111659	1.3333789072580462
0.4	1.5420107346364944	1.544482530617304	1.5486122593651872	1.5544150892093296
0.5	1.823236618073107	1.8273091055246455	1.8341193831132838	1.8437018387644573
0.6	2.1887805960676987	2.1951386303131555	2.2057807324625442	2.220775426389054
0.7	2.6648158229219474	2.6743770527180413	2.6903949338125925	2.7129941695811115
0.8	3.2858657279452137	3.2998380905284477	3.323265510914866	3.3563600284112325
0.9	4.095672991987155	4.1156183792085015	4.14908647984908	4.1964191716853865
1	5.148095231516944	5.175999390567274	5.222854817126482	5.289189551127658

TABLE V
RESULTS OF CASE 5 (DIFFERENT VALUES OF S_h)

X	s = 2	s = 3	s = 4	s = 5
0.1	1.0666129236604402	1.0994783376970565	1.1324505735876722	1.1655649840771904
0.2	1.1828209849651685	1.2744268034611266	1.3679959193645521	1.464178086914083
0.3	1.3397114847308156	1.5159322609431678	1.7029318115283956	1.9042773771447181
0.4	1.5415669175905258	1.8384064623067462	2.1713297910602147	2.5522788498521387
0.5	1.797298687391699	2.2671296074820617	2.8290763278568694	3.513624617739197
0.6	2.1192941185027223	2.8367705564931804	3.752351960739738	4.931601266857996
0.7	2.5231037459998724	3.5911148074485073	5.037631094211793	6.98791909600202
0.8	3.0273566235063094	4.583102955116582	6.8020394205773425	9.903649119521399
0.9	3.6537563782001836	5.874968580684206	9.183804454089717	13.94021358503357
1	4.427109748413025	7.538408819146187	12.342720181974983	19.400347084217266

A. CONCLUSION

The fractional thermal porous fin model mentioned above is a second-order non-linear ODE. This work uses HPM to illustrate the model solution numerically. It is shown that the HPM approach provides a straightforward, accurate, and suitable way to predict the consequences of heat dissipation in PFS when a thermionic system occurs. Here, the research on heat transmission is restricted to porous fins of finite length with insulated tips. We have two different situations that are susceptible to the fin's tip situation. The thermal gradients resulting from the dissimilarity of m with respect to the evolved heat energy and temperature propagation by varied values of α are depicted in Figure 1. Whereas, the thermal gradients that result from the differences in the evolution of heat energy and the propagation of temperature at different values are depicted in Figures 2 and 3. Here, it is determined that, as indicated in Figure 4 provided in [19]–[24], when impacted by m, S value increases, temperature drops quickly, and the fin quickly meets the ambient temperature. Figure 5 illustrates how S primarily influences thermal gradients. S is mostly attributable to the Darcy factor, which is the primary driver of heat transfer rate in this thermal system. Along with explaining the dissimilarity behavior, the results also provide an explanation for fin porosity and solidity in terms of the heat transfer rate with parameter kr [45], [46]. The percentage of porous fin to solid fin heat transmission rate differs in both scenarios as kr increases. The findings indicate that the values and variations of Da and Ra have a significant impact on the thermal dispersion of metallic Cu-Al-Ag porous structures. Figure 1 makes it clear that as the Darcy parameter decreases, the magnitude of thermal gradients and thermionic levels increases. As a result, the amount of dimensionless temperature decreases over the fin span. Here, it is determined that the S parameter mostly influences PFS because higher permeability results in increased convection and heat transferability. Greater heat transmission is possible at higher S values. Hence, this research concludes that porous finned structures or PFS are suitable for a variety of industrial uses, particularly in the electronics and biomedical sectors.

REFERENCES

[1] S. Saedodin and M. Shahbabaei, "Thermal analysis of natural convection in porous fins with homotopy perturbation method (HPM)," *Arab. J. Sci. Eng.*, vol. 38, no. 8, pp. 2227–2231, Feb. 2013, doi: https://doi.org/10.1007/s13369-013-0581-6.

[2] S. S. Chakrabarti, P. K. Das, and I. Ghosh, "RETRACTED: Thermal behavior of wet porous and solid fin–Experimental and analytical approach," *Int. J. Mech. Sci.*, vol. 149, pp. 112–121, Sep. 2018, doi: https://doi.org/10.1016/j.ijmecsci.2018.08.020.

[3] B. M. Al-Srayyih, S. Gao, and S. H. Hussain, "Effects of linearly heated left wall on natural convection within a superposed cavity filled with composite nanofluid-porous layers," *Adv. Powder Technol.*, vol. 30, no. 1, pp. 55–72, Jan. 2019, doi: https://doi.org/10.1016/j.apt.2018.10.007.

[4] P. Akbarzadeh and O. Mahian, "The onset of nanofluid natural convection inside a porous layer with rough boundaries," *J. Molecul. Liquid.*, vol. 272, pp. 344–352, Sep. 2018, doi: https://doi.org/10.1016/j.molliq.2018.09.074.

[5] Y. Joo and S. J. Kim, "Thermal optimization of vertically oriented, internally finned tubes in natural convection," *Int. J. Heat Mass Trans.*, vol. 93, pp. 991–999, Feb. 2016, doi: https://doi.org/10.1016/j.ijheatmasstransfer.2015.10.034.

[6] M. Hatami, A. Hasanpour, and D. D. Ganji, "Heat transfer study through porous fins (Si3N4 and AL) with temperature-dependent heat generation," *Energy Convers. Manage.*, vol. 74, pp. 9–16, Oct. 2013, doi: https://doi.org/10.1016/j.enconman.2013.04.034.

[7] S. E. Ghasemi, M. Hatami, and D. D. Ganji, "Thermal analysis of convective fin with temperature-dependent thermal conductivity and heat generation," *Case Stud. Therm. Eng.*, vol. 4, pp. 1–8, Nov. 2014, doi: https://doi.org/10.1016/j.csite.2014.05.002.

[8] R. Das, "Estimation of parameters in a fin with temperature-dependent thermal conductivity and radiation," *Proc. Institut. Mech. Eng. Part E J. Proc. Mech. Eng.*, vol. 230, no. 6, pp. 474–485, Mar. 2015, doi: https://doi.org/10.1177/0954408915575386.

[9] S. Kiwan and M. A. Al-Nimr, "Using porous fins for heat transfer enhancement," *J. Heat Trans.*, vol. 123, no. 4, pp. 790–795, Jul. 2000, doi: https://doi.org/10.1115/1.1371922.

[10] S. Kiwan, "Thermal analysis of natural convection porous fins," *Trans. Porous Media*, vol. 67, no. 1, pp. 17–29, Oct. 2006, doi: https://doi.org/10.1007/s11242-006-0010-3.

[11] A. -R. A. Khaled, "Investigation of heat transfer enhancement through permeable fins," *J. Heat Trans.*, vol. 132, no. 3, Dec. 2009, doi: https://doi.org/10.1115/1.4000056.

[12] S. Kiwan and O. Zeitoun, "Natural convection in a horizontal cylindrical annulus using porous fins," *Int. J. Numer. Methods Heat Fluid Flow*, vol. 18, no. 5, pp. 618–634, Jun. 2008, doi: https://doi.org/10.1108/09615530810879747.

[13] M. G. Sobamowo, O. M. Kamiyo, and O. A. Adeleye, "Thermal performance analysis of a natural convection porous fin with temperature-dependent thermal conductivity and internal heat generation," *Therm. Sci. Eng. Prog.*, vol. 1, pp. 39–52, Mar. 2017, doi: https://doi.org/10.1016/j.tsep.2017.02.007.

[14] M. Ghalambaz, E. Jamesahar, M. A. Ismael, and A. J. Chamkha, "Fluid-structure interaction study of natural convection heat transfer over a flexible oscillating fin in a square cavity," *Int. J. Therm. Sci.*, vol. 111, pp. 256–273, Jan. 2017, doi: https://doi.org/10.1016/j.ijthermalsci.2016.09.001.

[15] E. Cuce and P. M. Cuce, "A successful application of homotopy perturbation method for efficiency and effectiveness assessment of longitudinal porous fins," *Energy Convers. Manage.*, vol. 93, pp. 92–99, Mar. 2015, doi: https://doi.org/10.1016/j.enconman.2015.01.003.

[16] J. Ma, Y. Sun, B. Li, and H. Chen, "Spectral collocation method for radiative–conductive porous fin with temperature dependent properties," *Energy Convers. Manage.*, vol. 111, pp. 279–288, Jan. 2016, doi: https://doi.org/10.1016/j.enconman.2015.12.054.

[17] A. Moradi, A. P. M. Fallah, T. Hayat, and O. M. Aldossary, "On solution of natural convection and radiation heat transfer problem in a moving porous Fin," *Arab. J. Sci. Eng.*, vol. 39, no. 2, pp. 1303–1312, Sep. 2013, doi: https://doi.org/10.1007/s13369-013-0708-9.

[18] D. Bhanja, B. Kundu, and A. Aziz, "Enhancement of heat transfer from a continuously moving porous fin exposed in convective–radiative environment," *Energy Convers. Manage.*, vol. 88, pp. 842–853, Dec. 2014, doi: https://doi.org/10.1016/j.enconman.2014.09.016.

[19] M. Hatami, G. R. M. Ahangar, D. D. Ganji, and K. Boubaker, "Refrigeration efficiency analysis for fully wet semi-spherical porous fins," *Energy Convers. Manage.*, vol. 84, pp. 533–540, May 2014, doi: https://doi.org/10.1016/j.enconman.2014.05.007.

[20] S. Roy, K. G. Schell, E. C. Bucharsky, K. A. Weidenmann, A. Wanner, and M. J. Hoffmann, "Processing and characterization of elastic and thermal expansion behaviour of interpenetrating Al12Si/alumina composites," *Mater. Sci. Eng.*, vol. 743, pp. 339–348, Nov. 2018, doi:

https://doi.org/10.1016/j.msea.2018.11.100.

[21] M. G. Sobamowo, O. M. Kamiyo, and O. A. Adeleye, "Thermal performance analysis of a natural convection porous fin with temperature-dependent thermal conductivity and internal heat generation," *Therm. Sci. Eng. Prog.*, vol. 1, pp. 39–52, Mar. 2017, doi: https://doi.org/10.1016/j.tsep.2017.02.007.

[22] J. Ma, Y. Sun, and B. Li, "Simulation of combined conductive, convective and radiative heat transfer in moving irregular porous fins by spectral element method," *Int. J. Therm. Sci.*, vol. 118, pp. 475–487, May 2017, doi: https://doi.org/10.1016/j.ijthermalsci.2017.05.008.

[23] Y. Hirata, Y. Kinoshita, T. Shimonosono, and T. Chaen, "Theoretical and experimental analyses of thermal properties of porous polycrystalline mullite," *Ceram. Int.*, vol. 43, no. 13, pp. 9973–9978, May 2017, doi: https://doi.org/10.1016/j.ceramint.2017.05.009.

[24] X.-L. Ouyang, R.-N. Xu, and P.-X. Jiang, "Three-equation local thermal non-equilibrium model for transient heat transfer in porous media: The internal thermal conduction effect in the solid phase," *Int. J. Heat Mass Trans.*, vol. 115, pp. 1113–1124, Aug. 2017, doi: https://doi.org/10.1016/j.ijheatmasstransfer.2017.07.088.

[25] L. Wang, Z. Zeng, L. Zhang, H. Xie, G. Liang, and Y. Lu, "A lattice Boltzmann model for thermal flows through porous media," *Appl. Therm. Eng.*, vol. 108, pp. 66–75, Jul. 2016, doi: https://doi.org/10.1016/j.applthermaleng.2016.07.092.

[26] G. H. Tang, C. Bi, Y. Zhao, and W. Q. Tao, "Thermal transport in nano-porous insulation of aerogel: Factors, models and outlook," *Energy*, vol. 90, pp. 701–721, Oct. 2015, doi: https://doi.org/10.1016/j.energy.2015.07.109.

[27] T. Ozgumus and M. Mobedi, "Effect of pore to throat size ratio on thermal dispersion in porous media," *Int. J. Therm. Sci.*, vol. 104, pp. 135–145, Feb. 2016, doi: https://doi.org/10.1016/j.ijthermalsci.2016.01.003.

[28] X. Jin, L. Dong, Q. Li, H. Tang, N. Li, and Q. Qu, "Thermal shock cracking of porous ZrB 2 -SiC ceramics," *Ceram. Int.*, vol. 42, no. 11, pp. 13309–13313, May 2016, doi: https://doi.org/10.1016/j.ceramint.2016.05.040.

[29] V. Marinca and N. Herişanu, "The optimal homotopy asymptotic method for solving blasius equation," *Appl. Math. Comput.*, vol. 231, pp. 134–139, Mar. 2014, doi: https://doi.org/10.1016/j.amc.2013.12.121.

[30] L. Ali *et al.*, "A new analytical approach for the research of thin-film flow of magneto hydrodynamic fluid in the presence of thermal conductivity and variable viscosity," *ZAMM - J. Appl. Math. Mecha.*, vol. 101, no. 2, Aug. 2020, doi: https://doi.org/10.1002/zamm.201900292.

[31] M. H. Esfe, M. Bahiraei, H. Hajbarati, and M. Valadkhani, "A comprehensive review on convective heat transfer of

nanofluids in porous media: Energy-related and thermohydraulic characteristics," *Appl. Therm. Eng.*, vol. 178, p. 115487, May 2020, doi: https://doi.org/10.1016/j.applthermaleng.2020.115487.

[32] P. L. Ndlovu and R. J. Moitsheki, "Steady state heat transfer analysis in a rectangular moving porous fin," *Propul. Power Res.*, vol. 9, no. 2, pp. 188–196, Jun. 2020, doi: https://doi.org/10.1016/j.jppr.2020.03.002.

[33] Z. Shah, E. Bonyah, S. Islam, and T. Gul, "Impact of thermal radiation on electrical MHD rotating flow of Carbon nanotubes over a stretching sheet," *AIP Adv.*, vol. 9, no. 1, Jan. 2019, doi: https://doi.org/10.1063/1.5048078.

[34] Z. Shah, A. Dawar, S. Islam, I. Khan, and D. L. C. Ching, "Darcy-Forchheimer flow of radiative carbon nanotubes with microstructure and inertial characteristics in the rotating frame," *Case Stud. Therm. Eng.*, vol. 12, pp. 823–832, Sep. 2018, doi: https://doi.org/10.1016/j.csite.2018.09.007.

[35] Z. Shah, A. Dawar, E. O. Alzahrani, P. Kumam, A. J. Khan, and S. Islam, "Hall effect on couple stress 3D nanofluid flow over an exponentially stretched surface with Cattaneo Christov Heat Flux Model," *IEEE Access*, vol. 7, pp. 64844–64855, Jan. 2019, doi: https://doi.org/10.1109/access.2019.2916162.

[36] S. Nasir, Z. Shah, S. Islam, W. Khan, and S. N. Khan, "Radiative flow of magneto hydrodynamics single-walled carbon nanotube over a convectively heated stretchable rotating disk with velocity slip effect," *Adv. Mechan. Eng.*, vol. 11, no. 3, pp. 1–11, Mar. 2019, doi: https://doi.org/10.1177/1687814019827713.

[37] S. Nasir, Z. Shah, S. Islam, E. Bonyah, and T. Gul, "Darcy Forchheimer nanofluid thin film flow of SWCNTs and heat transfer analysis over an unsteady stretching sheet," *AIP Adv.*, vol. 9, no. 1, Jan. 2019, doi: https://doi.org/10.1063/1.5083972.

[38] R. Kumar, R. Kumar, S. A. Shehzad, and A. J. Chamkha, "Optimal treatment of stratified Carreau and Casson nanofluids flows in Darcy-Forchheimer porous space over porous matrix," *Appl. Math. Mechan.*, vol. 41, no. 11, pp. 1651–1670, Sep. 2020, doi: https://doi.org/10.1007/s10483-020-2655-7.

[39] R. Nawaz, Z. Hussain, A. Khattak, and A. Khan, "Extension of Optimal Homotopy Asymptotic Method with Use of Daftardar–Jeffery Polynomials to Coupled Nonlinear-Korteweg-De-Vries System," *Complexity*, vol. 2020, pp. 1–6, Mar. 2020, doi: https://doi.org/10.1155/2020/6952709.

[40] S. Iqbal, M. Idrees, A. M. Siddiqui, and A. R. Ansari, "Some solutions of the linear and nonlinear Klein–Gordon equations using the optimal homotopy asymptotic method," *Appl. Math. Comput.*, vol. 216, no. 10, pp. 2898–2909, Jul. 2010, doi: https://doi.org/10.1016/j.amc.2010.04.001.

[41] S. Iqbal and A. Javed, "Application of optimal homotopy asymptotic method for the analytic solution of singular Lane–Emden type equation," *Appl.*

Math. Comput., vol. 217, no. 19, pp. 7753–7761, Jun. 2011, doi: https://doi.org/10.1016/j.amc.2011.02.083.

[42] Hashmi, N. Khan, and S. Iqbal, "Numerical solutions of weakly singular Volterra integral equations using the optimal homotopy asymptotic method," *Comput. Math. Appl.*, vol. 64, no. 6, pp. 1567–1574, Sep. 2012, doi: https://doi.org/10.1016/j.camwa.2011.12.084.

[43] Hashmi, N. Khan, and S. Iqbal, "Optimal homotopy asymptotic method for solving nonlinear Fredholm integral equations of second kind," *Appl. Math. Comput.*, vol. 218, no. 22, pp. 10982–10989, Jul. 2012, doi: https://doi.org/0.1016/j.amc.2012.04.059.

[44] A. Javed, S. Iqbal, M. S. Hashmi, A. H. Dar, and N. Khan, "Semi-Analytical solutions of nonlinear problems of the deformation of beams and of the plate deflection theory using the optimal homotopy asymptotic method," *Heat Trans. Res.*, vol. 45, no. 7, pp. 603–620, Jan. 2014, doi: https://doi.org/10.1615/heattransres.2014007084.

[45] H. M. Younas, S. Iqbal, I. Siddique, M. K. A. Kaabar, and M. Kaplan, "Dynamical investigation of time-fractional order Phi-4 equations," *Opt. Quant. Elect.*, vol. 54, no. 4, Mar. 2022, doi: https://doi.org/10.1007/s11082-022-03562-6.

[46] M. Mustahsan, H. M. Younas, S. Iqbal, S. Rathore, K. S. Nisar, and J. Singh, "An efficient analytical technique for Time-Fractional parabolic partial differential equations," *Front. Phy.*, vol. 8, May 2020, doi: https://doi.org/10.3389/fphy.2020.00131.